Development of an interface between a plunger and an eccentric running track for a low-speed seawater pump

REVIEWED

ir. Joep Nijssen*, ir. Anton Kempenaar**, dr.ir. Niels Diepeveen**

Delft University of Technology, Department of Precision and Microsystems Engineering, Mekelweg 2, 2628CD Delft, The Netherlands*

Delft Offshore Turbine, Raam 180, Delft, The Netherlands**

E-Mail: J.P.A.Nijssen@tudelft.nl*

The DOT concept for offshore wind energy is a seawater hydraulic network where turbines are directly coupled to a centralized hydro-power platform. The essential missing component is a low-speed hydraulic pump that uses seawater as its hydraulic medium. This low speed hydraulic pump is currently being designed and tested by DOT, where novel machine components have been developed. This paper describes the development of an interface between an oval running track which is used as eccentricity to actuate a hydraulic piston. Several approaches have been performed as well as prototyping and validation steps. These steps as well as the design approach are presented in this work.

Keywords: Fluid power networks, positive displacement pump, Eccentricity, crank shaft replacement.
Target audience: (Sea)water Hydraulics, Offshore Industry, Design Process, Machine design.

1 Introduction

Advancements in wind turbine design mean records in terms of turbine size and power capacity continue to be broken. As blade length increases, the nominal rotation speed of wind turbines decreases asymptotically, and torque increases exponentially. In current industries were robust machines are used to handle large torques, hydraulic systems are usually preferred. Hence, the case for a compact hydraulic power train for a wind turbine is prevalent.

The Delft Offshore Turbine (DOT) concept makes use of a seawater hydraulic network where every wind turbine rotor is directly coupled to a positive displacement pump and electricity generation is centralized, creating an offshore hydro power plant /1/. Key design drivers are mass reduction and minimizing maintenance.

For much of the DOT concept, existing technology can be used as a basis. This also applies partially for the hydraulic drive train. Hydraulic piping and hydro power plant stations are mature technologies, and therefore do not need to be specifically developed. The essential missing component for the DOT drive train system is a pump that makes use of seawater as its hydraulic fluid. In previous studies /1/, it was determined that a positive displacement pump is the best option for the application in terms of torque to mass ratio, mechanical and volumetric efficiency. There is however no commercially available low-speed and high-torque positive displacement pump able to handle seawater as its hydraulic medium. Hence the decision was made in the spring of 2016 to develop such a machine inhouse. This paper focusses on an essential interface inside this pump: the conversion from rotary drive motion to linear piston motion. Two particular design solutions are described, including their prototyping and performance.

2 Design challenge

Previous work on the DOT approach made use of an existing second hand V44 Vestas wind turbine with a rated power output of 600 kW. The turbine was retrofitted with back-to-back oil and water hydraulic circuits to fundamentally prove the DOT approach at full scale /2-3/. Since the V44 Vestas was already available as a prototyping platform the choice was made to design the pump using the V44 Vestas nacelle geometry as design start condition. This restriction on the pump radius proved to be a major design challenge, so much so that the design pressure had to be restricted to 160 Bar. Also, other components in the hydraulic loop proved to be a limiting factor, thus restricting the design pressure to 160 Bar. A high-level overview of the DOT piston pump design can be seen in Figure 1. Lowering the design pressure meant lowering the input torque. As part of a follow-up project, a second pump segment is added to double the torque and make the pump design modular. Hence, the nominal volume flow of 1600 L/min and rated input torque 280 kNm are divided over the two modular segments.

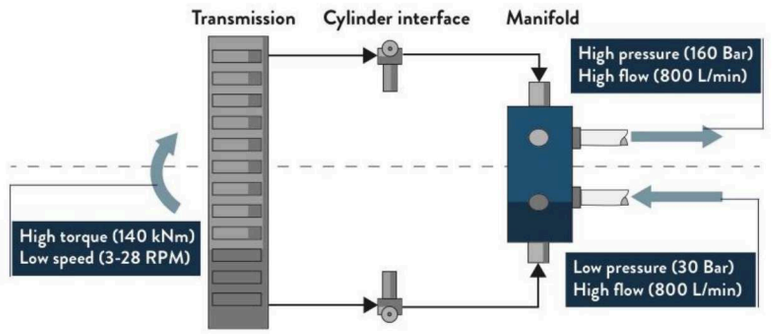

Figure 1: System architecture of one of the modular pump segments. The architecture can be divided into its three main interfaces. The transmission converts the input of the wind turbine into a higher rotational velocity. The cylinder interface converts an eccentric motion into a translation.

Another method to keep the pump dimensions within the restrictions was to increase the rotational speed of the wind turbine shaft from 28 RPM at max speed to 600 RPM by means of gearbox. This transmission is used to actuate an oval that is used as eccentric running track. This eccentric running track, called a wave generator ring (WGR), can be seen in Figure 2. The oval creates two strokes during every rotation, causing an effective speed of cylinder actuation at 1200 RPM. Hence, by lowering the design pressure, introducing a gear ratio and eventually adding a second module, the pump design is made sufficiently compact. The remaining challenge is the interface between the wave generator ring and the to-be actuated piston.

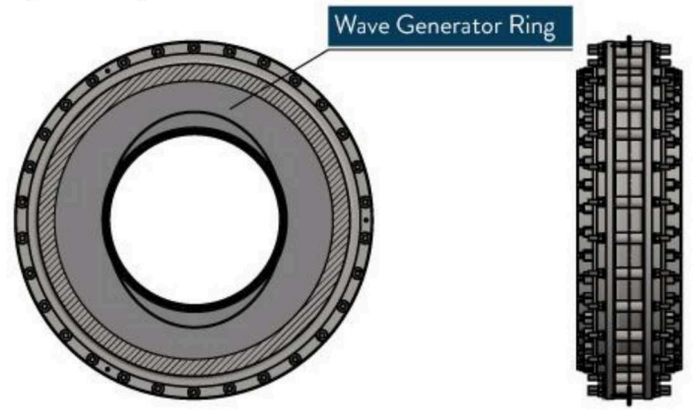

Figure 2: Overview of the drive and the placement of the wave generator ring.

3 Method

In this section the different approaches used to create the drive to plunger interface are discussed. The constraint on the pump dimensions meant that only a select number of design approaches could fit. Because of the nature of the problem, three approaches were originally discussed as possible solutions. These are sliding, rolling and fluid bearing interfaces. Of these approaches, both the sliding and rolling bearing interfaces are the most well-known and therefore have a lower risk during development. Both these approaches were designed and analysed. Both the sliding and rolling bearing interface design will be discussed.

3.1 Sliding bearing interface

A sliding bearing a basic commonly used tribological interface, found in a significant amount of machines /4/. As such, it proved to have great potential as the interface between the WGR and piston. To actuate the piston by as much of a pure translation as possible, an additional interface was designed between the WGR and piston. This interface consists of a combination of rollers, circular flexure and sliding bearing. These will be called inner rollers, waveband and slider bearing from this point onwards. The basic layout of this configuration can be seen in Figure 3.

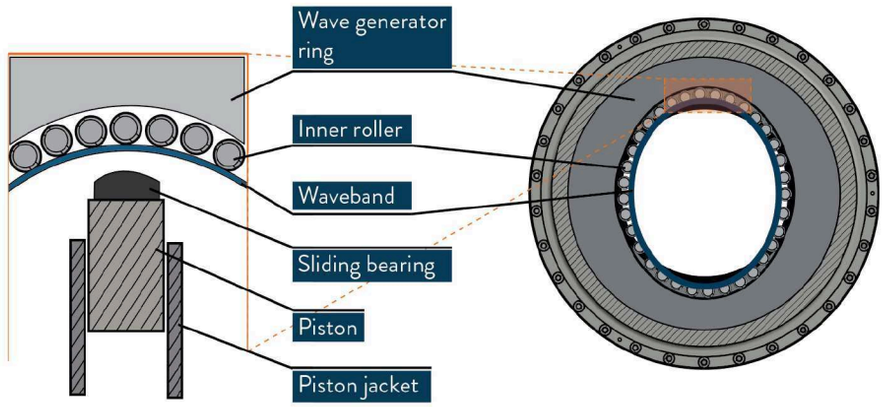

Figure 3: Sliding surface bearing approach. By adding additional rollers and a so-called waveband, the piston is actuated through almost pure translation.

By adding this additional rollers and flexure, a conversion from rotation to translation could be conceived. This created the following additional challenges:

- The design of a large single flexure with a deflection of 50 mm.
- Design of inner rollers which are subjected to high load cases up to 45 kN.
- Design of a stable sliding bearing with a lifetime of 6 months.

Since the dimensions were limited, the max size of the sliding bearing and its possible sacrificial material was therefore also limited. These main objectives were the goal of detail designing of this principle.

3.1.1 Detail design: sliding bearing

The limiting dimensions meant only 10 mm of sacrificial material was available for the sliding bearing. With the goal of 6-month operational lifetime, this means a wear rate of the sliding bearing of 2.3 μm per hour. This is at operational conditions at 1200 RPM/160 Bar. To obtain a low wear rate with a sliding bearing, the PV-value has to be low. Because of the configuration of the waveband and sliding bearing, there still exists an oscillating horizontal motion between the waveband and bearing. This oscillating motion occurs over a distance of 50 mm, with an average velocity of 1.87 m/s. Next to this is the horizontal stroke of the cylinder caused by the deflection of the waveband. To obtain the desired flow, with the chosen cylinder dimensions, this stroke is equal to 50 mm. The geometry of the sliding bearing is designed such as to maximize the amount of surface area, therefore lowering the contact pressure on the bearing with the waveband. The surface area of the final slider bearing is equal to 785 mm^2. With this surface area the trajectory made by the sliding bearing as well as its final design can be seen in Figure 4.

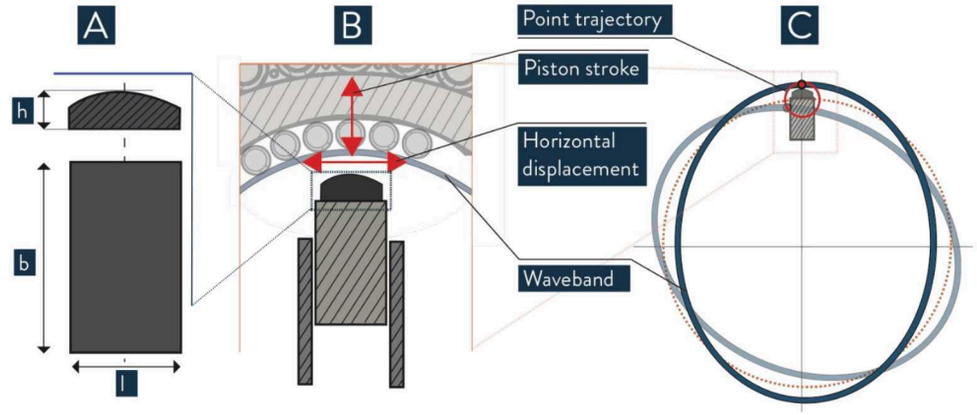

Figure 4: (A) The basic geometrical dimensions of the sliding bearing where h=10mm, b=150mm and l=70mm. The rounded corners cause the total surface area to be 9500 mm^2. (B) The piston and its stroke being equal to 50mm and its horizontal displacement being equa

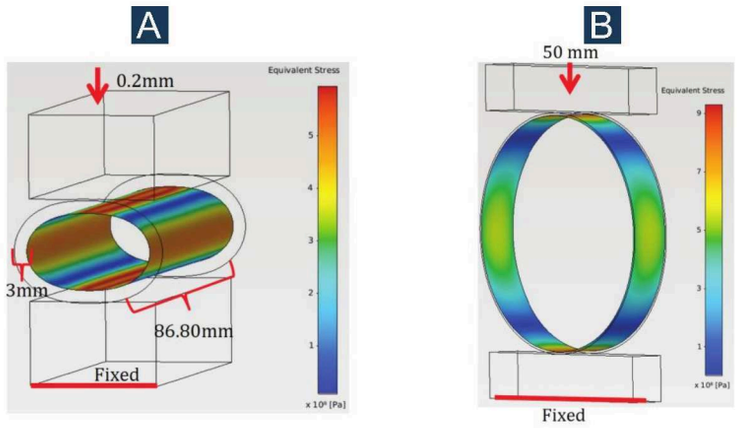

Figure 5: (A) The FEM modelling of the inner roller with a pre-compression of 0.2 mm. Its occurring Von Mises stress is 545 MPa. (B) The FEM model of the waveband at 50 mm deflection. Its maximum occuring Von Mises stress is 910 MPa.

Since the waveband and inner rollers are fundamentally circular flexures, their occurring stresses can be predicted with high accuracy using a finite element approach. Both were modelled using Comsol Multiphysics with a geometrical nonlinear approach to determine its compliance behaviour. Both were modelled with a linear elastic material model using a Youngs modulus of 210E9 Pa. To transfer the motion as well as the forces from the wave generator ring to the piston, the inner rollers had to be pre-compressed. 0.2 mm compression created the desired traction between these components. The load cases and resulting Von Mises stresses of the individual modelling of both the waveband and inner rollers can be seen in Figure 5. The load capacity of the waveband at max deflection

of 50 mm is equal to 3000 N, which can be used as a validation of the FEM model. The material used to produce both components is heat treated 100Cr6 with a yield stress of 2500 MPa.

3.2 Roller bearing interface

Another fundamental approach to solving this interface problem is by using a roller bearing. The main limitation on the choice of bearing for the cylinder interface was the available dimensions. In this case a maximum design space height of 50 mm was available for the roller bearing. This has significantly limits the bearing diameter. The main advantage of this kind of interface is that the contact area is limited to a line contact, and therefore no additional mechanism is needed to convert the rotation into translation as was done for the sliding bearing. Roller bearings have also been widely investigated and lifetime calculations are in general reliable, and described in the ISO 281:2007 norm /6/.

3.2.1 Detail design: roller bearing

The choice was made to make use of the SKF NNCF 5004 CV, which is the largest double row cylindrical bearing available able to fit within the design space. This bearing has a basic dynamic load rating of 52.3 kN with a reference speed of 8500 RPM. The final cylinder interface design can be seen in Figure 6.

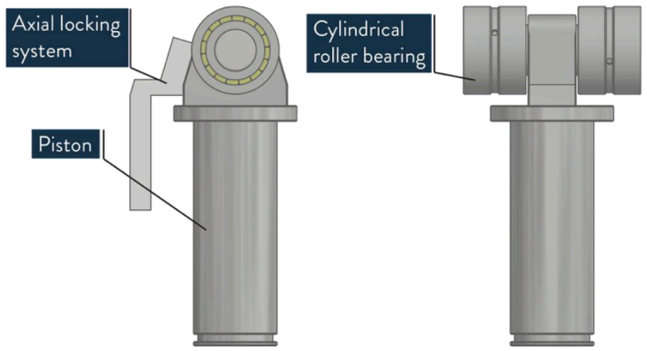

Figure 6: Configuration of the roller bearing on top of the piston. The axial locking system prevents rotation arund the axis.

At 160 bar, the static load on the piston is 45.2 kN, assuming an equally distributed load on each roller bearing of 22.6 kN. Taking into account the dimensions of the WGR as well was the dimensions of the roller bearing gives a rotational velocity of 8100 RPM. An indication of bearing lifetime was calculated using the following equation:

$$L10h = \frac{10^6}{60 \cdot n} \cdot \left(\frac{C}{P}\right)^3 \tag{3}$$

Which is a basic life rating indication at 90% reliability /8/ in hours. Here, C equals the basic dynamic load rating of the bearing in Pa, P is equal to the load per bearing in Pa and n equals the rotational velocity of the bearing in RPM. The calculated lifetime at previously mentioned conditions is 40 hours, which is an accepted risk at this point of pump development. It however also directly shows the severe limitation of the roller bearing interface. The axial locking system was added to minimize the effect of axial rotations, which could drastically increase the load on a single bearing thereby shortening its limited lifetime even further.

4 Results

Both interfaces were prototyped either partially to test critical components, or in full. The results of their performance will be discussed in this section. In all cases no additional lubrication is used. The environment where this interface is part of will be constantly contaminated with seawater and as such, no stable lubrication can be used. The objective is therefore to find a interface that also functions without the use of lubrication.

4.1 Sliding bearing interface

For the sliding bearing interface, the following three cases were identified as being critical to its performance. These are as follows:

- Lifetime of the sliding bearing/waveband interface.
- Lifetime of the waveband
- Lifetime of the inner roller

These three cases will therefor all be discussed.

4.1.1 Sliding bearing material

To determine the wear rate of the sliding bearing/waveband interface a pin-on-disk measurement /4/ was performed for several high potential materials to determine their wear rate, change in friction coefficient and temperature change. The test setup can be seen in Figure 7. Two materials, AS PC04 and ZL1500T, were tested in a scaled loading condition. ZL1500T is a modified PEEK material, while AS PC04 is a carbon based composite material.

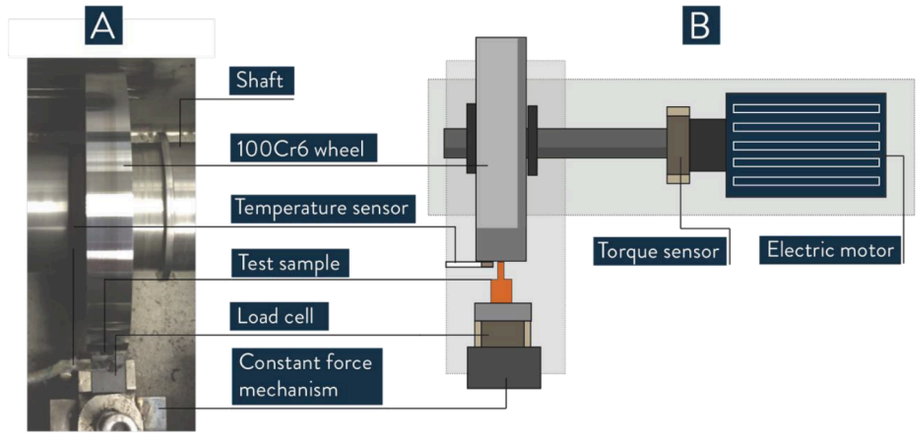

Figure 7: (A) Pin-on-disk test setup used to determine the wear properties of the sliding bearing materials. A 100Cr6 disk is used as running track. The constant force mechanism guarantees that the pin is laoded with a constant load.

The pin-on-disk measurement was performed for 90 minutes with a sample rate of 5 Hz to gain some insight on the desired properties. A load of 350 N was applied on the test samples with a surface of 6.25 mm^2 to obtain an equal load condition as the full scale sliding bearing. The displacement measurements were filtered using a low-pass Butterworth filter. The disk is made from 100Cr6 with a hardness of 45 HRC and a roughness of 0.3 Ra. The friction coefficient was determined by the balance of load case and output of the torque sensor. The result of this measurement can be seen in Figure 8. The main issue with both materials is that the temperature does not reach a steady state temperature, which is destructive for sliding bearings /6/. The wear rate for the PC04 is also significant, causing it to fail in terms of lifetime. The main cause of this is the high velocity.

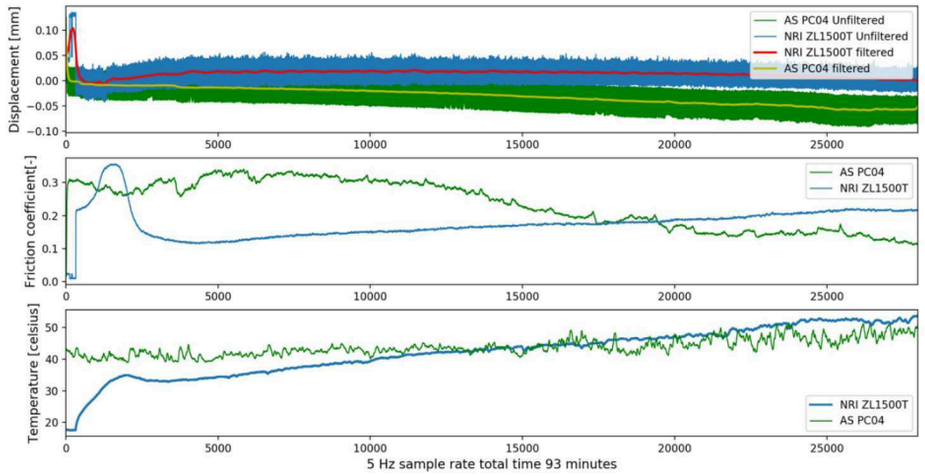

Figure 8: The tribology properties of both AS PC04 and NRI ZL1500T. In all cases the friction, wear in terms of displacement towards the wheel and temperature is shown.

4.1.2 Waveband lifetime

The waveband was prototyped using 100Cr6 which was heat treated to increase the yield strength of the material. The waveband fabricated by turning a large cylinder to its final dimensions of 5 mm thickness. Since the waveband is an unconventionally large flexure /7/, it was also measured to confirm the finite element model in terms of the occurring stresses as well as its force-deflection behaviour. A Swick test bench was used to actuate the waveband with a max load of 1000 N, and a max stroke of 100 mm, to gain an indication of the initial behaviour of the waveband. The test setup can be seen in Figure 9.

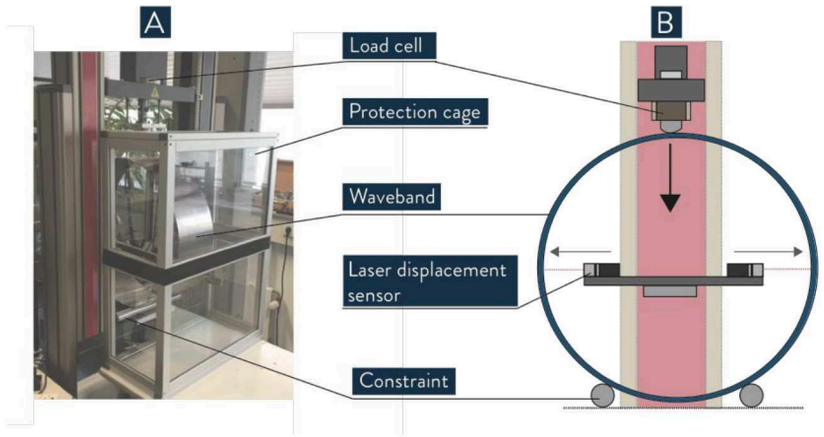

Figure 9: (A) The test setup used to measure part of the force-deflection curve of the waveband. (B) overview of the measurement setup. The waveband is imposed on the beams on the bottom and actuated on the top to create a stable constraint situation.

The displacement of the waveband was measured using an optoNCDT ILD 1401-100 laser displacement sensor. The test setup and results of the measurement can be seen in Figure 10. By linearly extrapolating the measurements made, a maximum error of 3% between the measurement and FEM model was obtained. The FEM can therefore predict the occurring stress state with a relative high degree of accuracy.

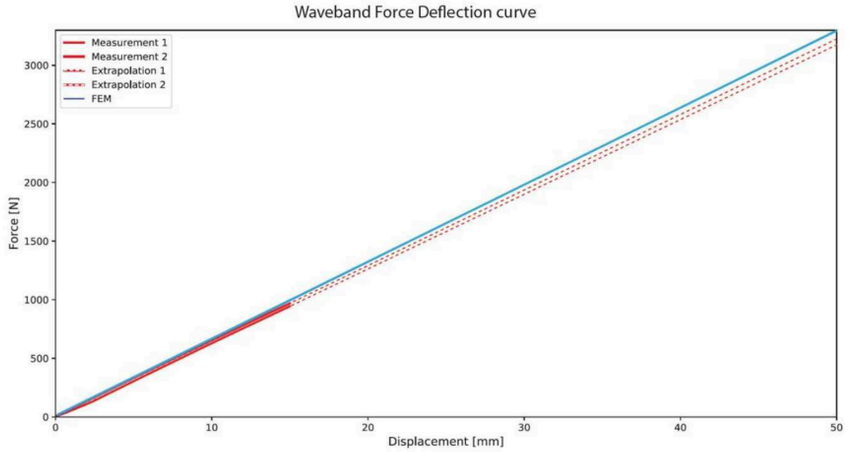

Figure 10: (A) Resulting force-deflection of the waveband. Because of the limitations of the test bench only 30% of the force deflection curve could be measured. By linearly extrapolating the results a 3% error was achieved between the waveband and fin

4.1.3 Inner roller lifetime

The inner roller lifetime is greatly dependent on its load case and the occurring stress level. Because the absolute deflection of the inner rollers is significantly smaller then for the waveband, it can still be modelled as a geometric linear model. Therefore, is its lifetime is further investigated by modelling the inner rollers in the entire system with a finite element approach. The resulting load case can be seen in Figure 11.

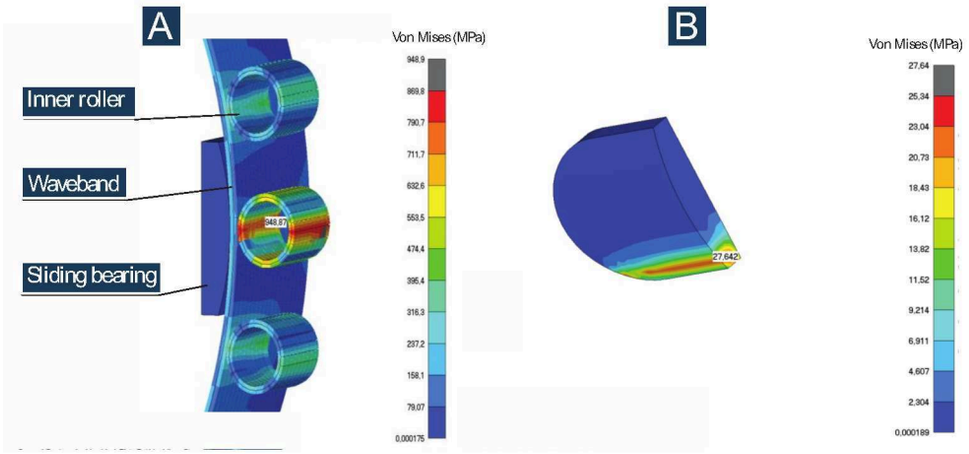

Figure 11: Load case modelled with a finite element approach. In the figure the maximum occurring compressive stress is visualized. (B) shows that the von mises stresses occurring on the sliding bearing are lower then designed for.

Although the Von Mises stresses are significantly higher but still acceptable, it's the circumferential stresses causing the very limiting lifetime. The circumferential stress range occurring at the inner rollers exceeds 2000 MPa. Since these are not contact stresses, this is not an allowable stress range. This severely limits their lifetime and therefore not making it a suitable mechanism for the desired loading conditions. What should also be noted that is that the pressure on the sliding bearings is significantly lower with only a max of 27.64 MPa, instead of the design value of 56 MPa. This is caused by the compliance of the waveband and inner rollers.

4.2 Roller bearing interface

Since the roller bearings are standardized components and the lifetime calculations determined a very limited but critical lifetime, the choice was made to make a simple test setup to validate this. The test setup can be seen in Figure 12.

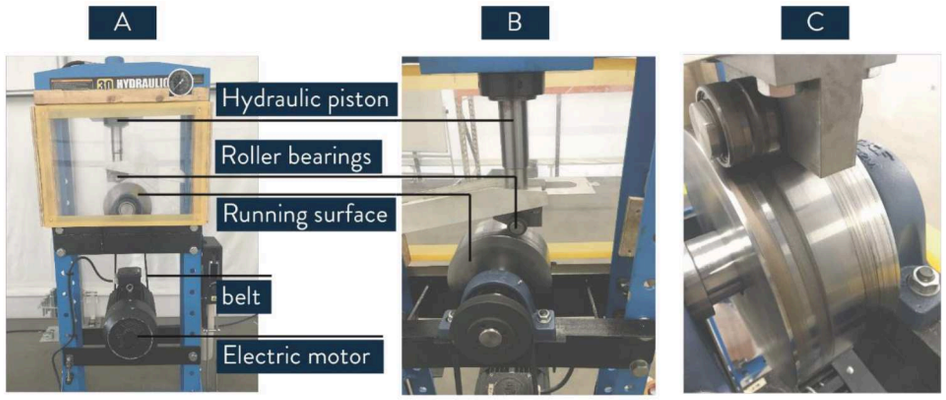

Figure 12: (A) Test setup used to test performance of the cylindrical roller bearing. (B) close up of running surface and the method of actuating the bearing onto the running surface. (C) wear damage caused by the cylindrical bearing on the running surf

The test setup is designed such that both the pressure on the roller bearings as well as the revolution velocity of the WGR can be achieved. The Running track is made from 100CR6 with a hardness of 58 HRC. The hydraulic piston is used to apply an external load up to 50,000 N.

The roller bearing was initially loaded at 5000 N, which is 10% of max capacity and the running track was slowly increased to its max velocity of 18 m/s which corresponds to an actuation velocity of 900 RPM of the running track. Every interval increase of 100 RPM was performed for 300 seconds. It was found that at a load of 5000 N with a rotational velocity of 900 RPM, the bearing both caused destructive damage to the internal cylindrical rollers of the bearing. This was seen by steel dust being emitted from the internal rollers, meaning destructive failure of the inner cylinders. Internally the roller bearing was not up to the specified requirements and performed worse than its expected calculated lifetime. Additionally, the loads were so significant that permanent damage was caused on the running surface as seen in figure 12.C.

5 Conclusion & outlook

DOT is developing a low-speed positive displacement pump for seawater. Arguably the most critical interface of this pump is there where the conversion from rotary drive motion to linear plunger motion takes place. Two solutions for this interface have been developed and tested, namely specific types of slider and roller bearings. For the slider bearing both the speed and stress were too large. For the roller bearing the load also proved far too great for the allowable bearing diameter.

By not having a rigid body mechanism between the wave generator ring and piston, the piston is subjected to a shear load. The effects of this phenomena on the piston and its lifetime will be discussed in future work.

Since both solutions have proven to be inadequate an alternative is required. Therefor the next step is to develop a hydrostatic bearing /8/. Although such a bearing would introduce additional volumetric losses, mechanical losses are less, and wear is minimal. A significant challenge for this particular hydrostatic bearing is the required material compliance to follow the shape of the ellipsoidal running track.

6 Acknowledgements

The research presented in this paper was part of the DOT500 ONT project, which was conducted by DOT in collaboration with the TU Delft and executed with funding received from the *Ministerie van Economische zaken* via *TKI Wind op Zee, Topsector Energie*.

References

/1/ Diepeveen, N.: On fluid power transmission in offshore wind turbines, PhD thesis, Technical University of Delft, August 2013

/2/ Mulders, S., Diepeveen, N., Van Wingerden, J.: Control design and validation for the hydraulic DOT500 wind turbine, Proceedings of the 11th International Fluid Power Conference. RWTH Aachen, 2018.

/3/ Diepeveen, N., Mulders, S., van der Tempel, J., Nijssen, J.P.A.: Field tests of the DOT500 prototype wind turbine, Proceedings of the 11th International Fluid Power Conference. RWTH Aachen, 2018.

/4/ Van Beek, A.: Advanced Engineering Design Lifetime performance and reliability, Engineering-abc, The Netherlands, 2015.

/5/ Stachowiak, G., Batchelor, A.: Engineering Tribology, Butterworth-Heineman, United States, 2005.

/6/ ISO281:2007, ISO 281:2007: Roller bearings, Dynamic load rating and rating life, 2007-02, International Organization for Standardization, Geneva, Switzerland. https://www.iso.org/standard/38102.html

/7/ Howell L.: Compliant Mechanisms, Springer, Unites States, 2003.

/8/ Van Ostayen, R.A.J.: The Hydro-support: An Elasto-Hydrostatic Thrust Bearing with Mixed Lubrication, PhD Thesis, 2002.